

Parameter identification of claystone formations in underground laboratories

Roger Schlegel, Petr Vymatil, Johannes Will^{1*},
Michael Jobmann, Mirko Polster, Michael Breustedt²

¹ Dynardo – Dynamic Software and Engineering GmbH, Weimar

² DBE TECHNOLOGY GmbH, Peine

Summary

In search of suitable disposal sites for hazardous waste in underground laboratories, heating experiments are carried out to investigate thermal-hydraulic-mechanical interactions. In these experiments, the time depending changes of temperature, pore pressure and stress fields can be measured as a result of applying heat energy to rock formations. The DBE TECHNOLOGY GmbH developed, in collaboration with the Dynardo GmbH, simulation models which can be used to understand these interactions within the claystone formation. An important part of this development is the model calibration based on measurement results. The heating experiment was simulated by the use of a Thermal-Hydraulic-Mechanical (THM) coupled, 3-dimensional finite element analysis with ANSYS[®] and multiPlas. In this case, special routines for poroelasticity theories, thermal-hydraulic coupling and hydraulic-mechanical coupling were developed in isotropic or anisotropic claystone formations and implemented in ANSYS[®]. The optimization software optiSLang[®] was used for the sensitivity analysis and the parameter identification. The complexity of the thermal-hydraulic-mechanical phenomena required a number of about 30 model parameters. Decisive conditions for the successful calibration between measurement and simulation of such a complex task are, on the one hand, high-performance algorithms and filtering strategies for coping with large parameter spaces available in optiSLang[®], and, on the other hand, the short calculation time achieved by using ANSYS[®] and multiplas.

Keywords: underground laboratories, claystone, thermal-hydraulic-mechanical coupling, parameter identification

* Contact: Dr.-Ing. Roger Schlegel, Dynardo GmbH, 99423 Weimar, Steubenstraße 25, Roger.Schlegel@dynardo.de

1 Project aim

The aim of the computational analysis was the Thermal-Hydraulic-Mechanical (THM) coupled recalculation of a heating experiment using a 3-dimensional simulation model. It should be shown that the THM interactions within the claystone can be simulated with reasonable accuracy and the simulation results can be compared with the available measurements. Using a sensitivity analysis, the essential interconnections between the measured end results and the input parameters should be identified.

2 Finite element simulation of heating experiments in underground laboratory

The heating experiment was simulated using 3-dimensional finite element analysis (ANSYS® and Multiplas). The initial state, i.e. the in-situ stress, pore pressure and temperature conditions were activated by means of initial material properties and boundary conditions. The excavation of the tunnel was simulated by deactivation the corresponding element areas. Here, the increase of permeability was included in the excavation-damaged zone. Subsequently, a nonlinear coupled THM finite element analysis of each heating period of the experiment was conducted. Figure 1 shows a section of the FE model.

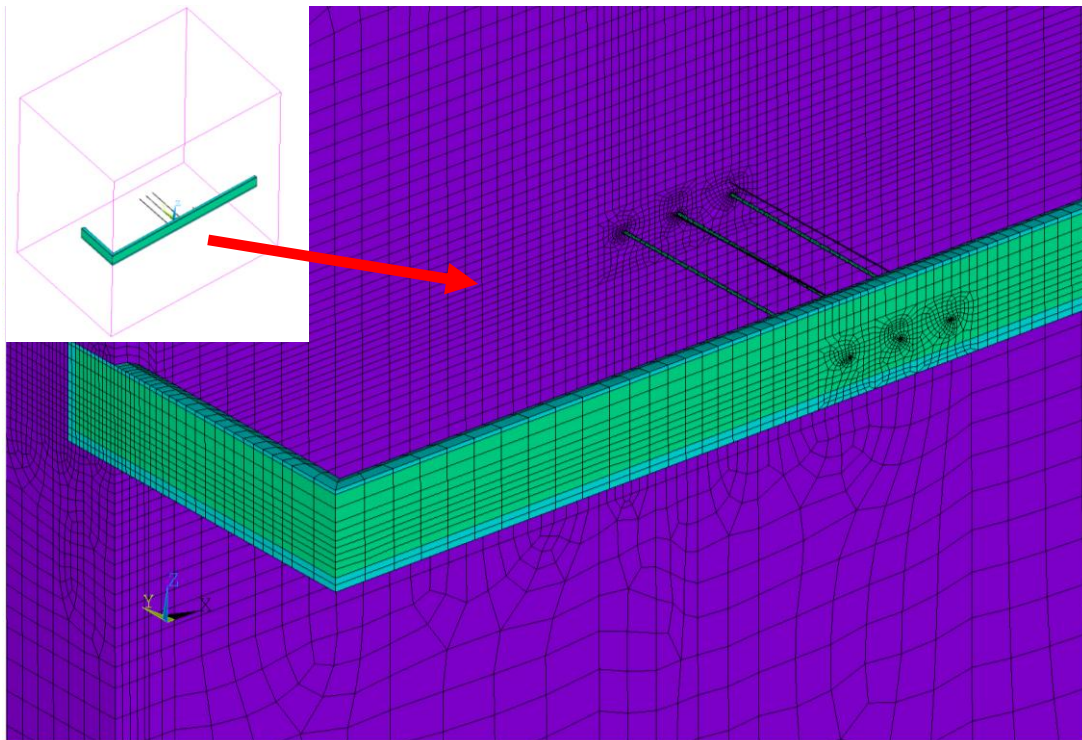


Figure 1: FE-mesh of structure, section

The experiment was carried out in three periods with a corresponding increase of temperature output of the three heaters. Figure 2 shows the evolution of the three heating periods.

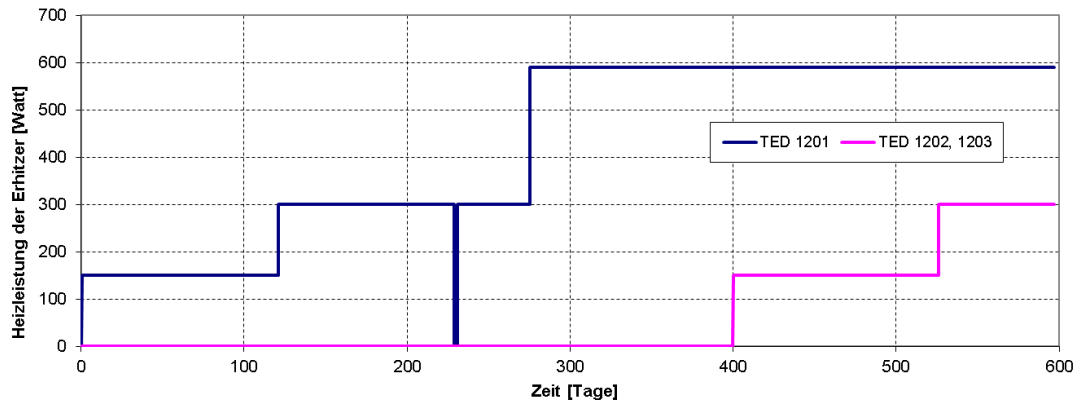


Figure 2: Periods of heating (Andra, 2005)

3 Modeling strategy of the claystone

An anisotropic material model containing the coupling of the isotropic Mohr-Coulomb model (rock matrix) and the anisotropic Mohr-Coulomb model (bedding plane) was generated with multiPlas and ANSYS®. This model was used for the continuum mechanical modeling of the claystone (Callovo-Oxfordian). The material model considers different behavior of the claystone in the pre and post fracture zone. Using optiSLang®, the FE model was parameterized.

4 T-H-M coupled calculation of the heating experiment

The simulation of the construction process (tunneling) was conducted in the mechanical analysis by deactivation and activation the corresponding element areas. After deactivation of the claystone elements within the considered section, in a further step, the cladding elements of the tunnel were activated using the parameters of the shotcrete. The elements in the air and heater areas remained deactivated. The fracture sections were adapted to the FE mesh. For the thermal and hydraulic analyses, the construction process was considered analogously. Instead of activating and deactivating, the material properties of the respective elements of claystone to air and then air to shotcrete or heater were modified. For the thermal-hydraulic-mechanical simulation, the following non-linear interactions between anisotropic thermal, hydraulic and mechanical material properties were considered:

- T-H coupling: the updating of the pore water pressure due to temperature changes and the temperature dependence of the hydraulic conductivity,
- T-M coupling: the influence of mechanical stress and deformation state by thermal expansion,
- H-M coupling: updating the effective stress due to pore water pressure changes and
- M-H coupling: the dependence of the hydraulic conductivity in comparison to the stress state and the vector of plastic strains as well as the updating of the pore water pressures due to stress changes

The change of the pore water pressure P is due to the changes of fluid volume ζ , volumetric expansion ε_v and temperature T according to the following constitutive equation

$$\frac{1}{M} \frac{\partial P}{\partial t} = \frac{\partial \zeta}{\partial t} - \alpha \frac{\partial \varepsilon_v}{\partial t} + \beta \frac{\partial T}{\partial t} \quad (1)$$

with M Biot-modulus [Pa],
 α Biot-Coefficient [-]

Here, the undrained, thermal coefficient is defined as

$$\beta = 3[\alpha_s(\alpha - n) + \alpha_{f, fact} \alpha_f n] \quad (2)$$

with α_s thermal coefficient of expansion of the claystone matrix [1/K]
 α_f temperature-dependent, volumetric coefficient of expansion of pore fluids [1/K],
 $\alpha_{f, fact}$ scaling factor of α_f [-]
 n porosity [-]

The hydraulic conductivity of the claystone is formulated as a function of temperature and the stress-strain state. Here, the anisotropic permeability is dependent on the stress state, the vector of the plastic strain and the orientation of the bedding plane. The permeability coefficient is defined as

$$K_i = \frac{k_i \times \rho_f \times g}{\mu_w(T)} \quad \text{for } i=x, y, z \quad (3)$$

with k_i permeability
 $\mu_w(T)$ temperature-dependent, dynamic viscosity of water

The permeability depends on the state of stress σ and the vector of the plastic strain ε^{pl} . according to the following equation

$$k_i = k_{\sigma, i} + k_{\varepsilon, i} \quad \text{für } i=x, y, z \quad (4)$$

The function for permeability in the horizontal directions x, y (parallel to the bedding plane) $k_{\sigma,p} = k_{\sigma,x} = k_{\sigma,y}$, derived in Millard (2005), is defined as

$$k_{\sigma,x} = k_{\sigma,y} = k_{\sigma,p} = k_{0,p} \times \left(\frac{\sigma_z}{\sigma_0} \right)^{-n_p} \quad (5)$$

with σ_z normal stress at bedding plane
 $\sigma_0 = 1$ MPa
 $k_{0,p}, n_p$ parameter.

The function of permeability in the vertical direction z (normal at bedding plane) $k_{\sigma,n} = k_{\sigma,z}$, derived in Millard (2005), is defined as

$$k_{\sigma,z} = k_{\sigma,n} = k_{0,n} \times \left(\frac{\sigma_{m,h}}{\sigma_0} \right)^{-n_n} \quad (6)$$

with $\sigma_{m,h} = (\sigma_x + \sigma_y) / 2$
 $k_{0,n}, n_n$ parameter.

The function $k_{\varepsilon,i}$ is defined for directions $i = x, y, z$

$$k_{\varepsilon,x} = k_{\varepsilon} \times (\varepsilon_y^+ + \varepsilon_z^+) \quad k_{\varepsilon,x} \leq k_{\varepsilon,\max} \quad (7)$$

$$k_{\varepsilon,y} = k_{\varepsilon} \times (\varepsilon_x^+ + \varepsilon_z^+) \quad k_{\varepsilon,y} \leq k_{\varepsilon,\max} \quad (8)$$

$$k_{\varepsilon,z} = k_{\varepsilon} \times (\varepsilon_x^+ + \varepsilon_y^+) \quad k_{\varepsilon,z} \leq k_{\varepsilon,\max} \quad (9)$$

with $\varepsilon_i^+ = \varepsilon_i^{pl}$ for $\varepsilon_i^{pl} \geq 0$ and $\varepsilon_i^+ = 0$ for $\varepsilon_i^{pl} < 0$

5 Sensitivity analysis

In the sensitivity analysis, the material parameters (including the parameters of the coupling dependencies) were varied within physically possible parameter limits. It should be investigated which of the material parameters have a relevant and physically understandable context for a comparison with the experimental results. For analyzing, data of temperature and pore water pressure from a total of 17 measurement points were available. Due to the many uncertainties of the Tunnel excavation and the installation of the instruments, model calibration and parameter identification were limited to the heating experiment. Here, not the total pore water pressure but the pressure differentials and gradients as results of the heating and applied to the beginning of the heating periods were considered (see Figure 3).

For the sensitivities evaluation of the relative pore water pressures, discrete values at certain times were used. The selection of these response variables made an evaluation of the sensitivity at the beginning and the end of the respective heating phases as well as at the time of reaching the maximum pore water pressure possible. Important results of the sensitivity analysis could be derived from the

CoP values (Coefficients of Prognosis), which show the significance of the input parameters. In order to determine the CoP values, the MOP (Metamodel of Optimal Prognosis) is generated by optiSLang showing the best correlation between the variation of response variables and input variables. optiSLang filters out automatically unimportant input parameters. This strategy allows optiSLang, with a minimal number of designs, to identify efficiently the significant input parameters even in large parameter spaces. Thereby, also non-linear correlations are detected.

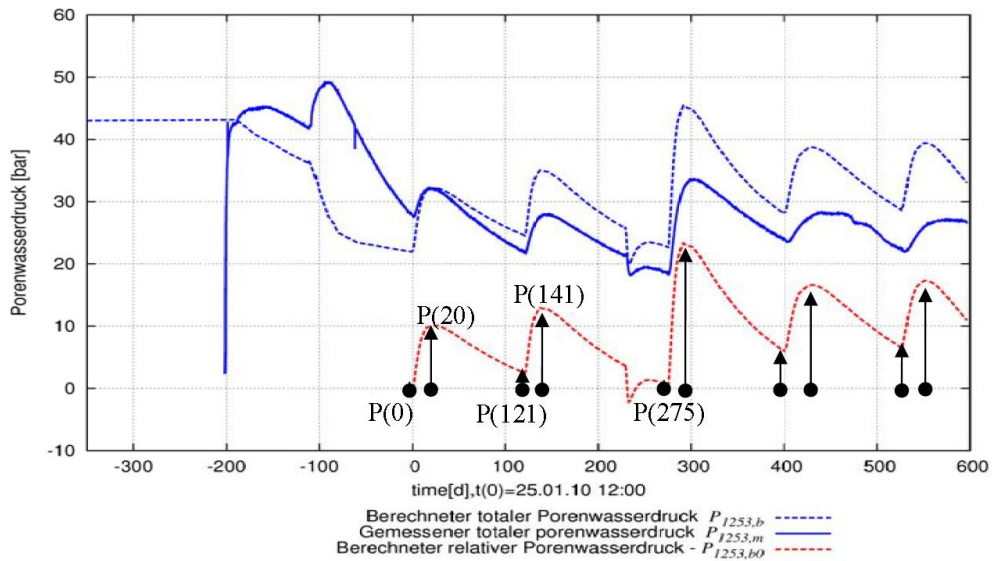


Figure 3: Relative pore water pressures for parameter identification

Figure 4 to Figure 6 are examples of the measurement point 1251 showing the CoP values of the input variables for the relative pore pressures at the times $t = 0$ (start of heating), $t = 20$ days (reaching the maximum pore water pressure) and $t = 121$ days (end of the heating phase 1).

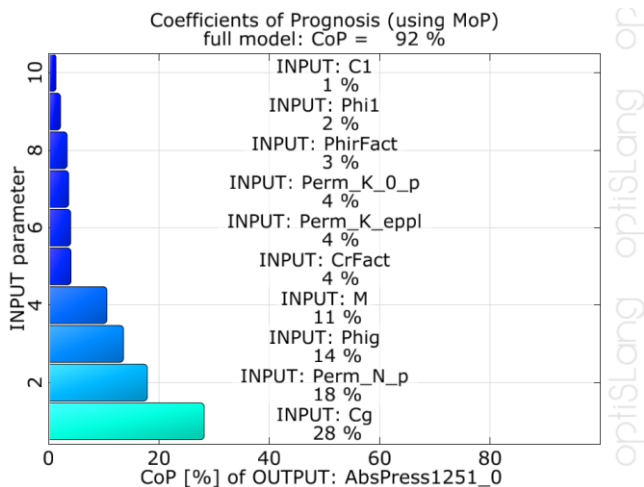


Figure 4: CoP relative pore pressure at time $t = 0$, the measuring point in 1251

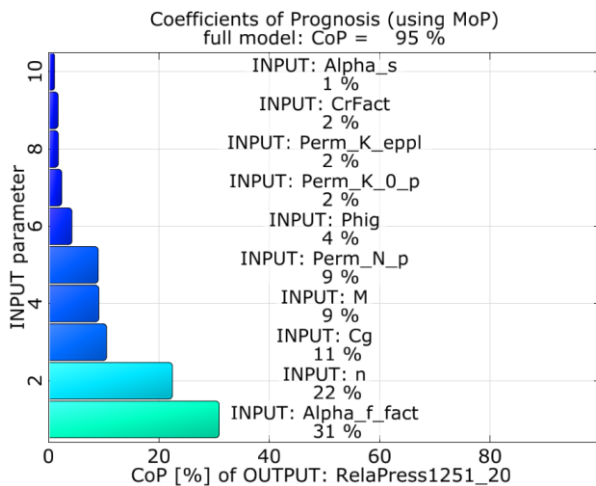


Figure 5: CoP relative pore pressure at time $t = 20$ days, measurement point 1251

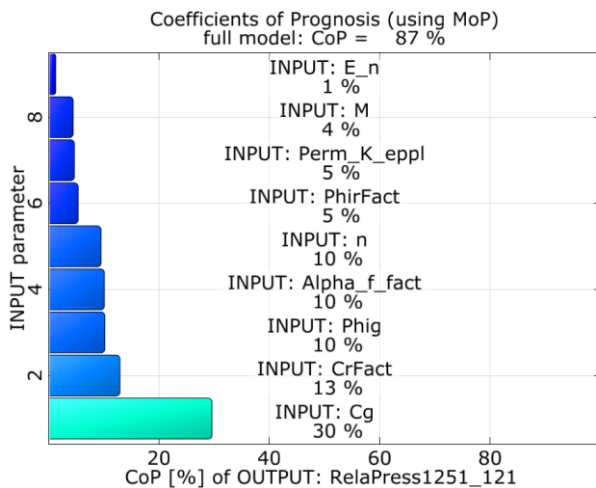


Figure 6: CoP relative pore pressure at time $t = 121$ days, measurement point 1251

Evaluating the CoP values at all measuring points, it can be stated that at time $t = 0$ (before start of heating), especially the following input variables influence the pore water pressure:

- Perm_N_p, Perm_K_0_p - the permeability function of H-M coupling constants
- CG and phig - strength parameters (cohesion and friction angle) of the claystone
- M – Biot modulus and

During the heating phases of the experiment especially the following input variables influence the pore water pressure:

- Alpha_f_fact - factor of the temperature-dependent volumetric expansion of the pore fluid (T-H coupling)
- n - porosity (T-H coupling)
- Perm_N_p, Perm_K_0_p, Perm_N_n, Perm_K_0_n - permeability function of the H-M coupling constants,

- CG and ϕ_{ig} - strength parameters (cohesion and friction angle) of the claystone and
- M – Biot modulus

It can be seen that the pore water pressure increase at the beginning of each heating phase, is in particular influenced by the value α_f and n (values of the TH-coupling). The subsequent decrease of pore water pressure values, however, shows a significant correlation to the strength characteristics of the claystone (c_g and ϕ_{ig}). This is an indication for the pore water pressure decline being particularly caused by stress redistribution, change of permeability and drainage effects. The high total CoP values of the individual response variables of $> 85\%$ emphasize the high plausibility of the main physical phenomena by the identified correlation. Furthermore, by comparing the scattering ranges of the calculated values with the time variations of the measurement results (see Figure 7), evaluations about the model quality and adjustability of the numerical model with the experimental results could be made. If the scattering range of the simulation model includes the measured evolution of parameters, a successful comparison within the selected parameter limits is possible. Figure 7 shows the correctness of this evaluation starting from the beginning of the experiment ($t = 0$).

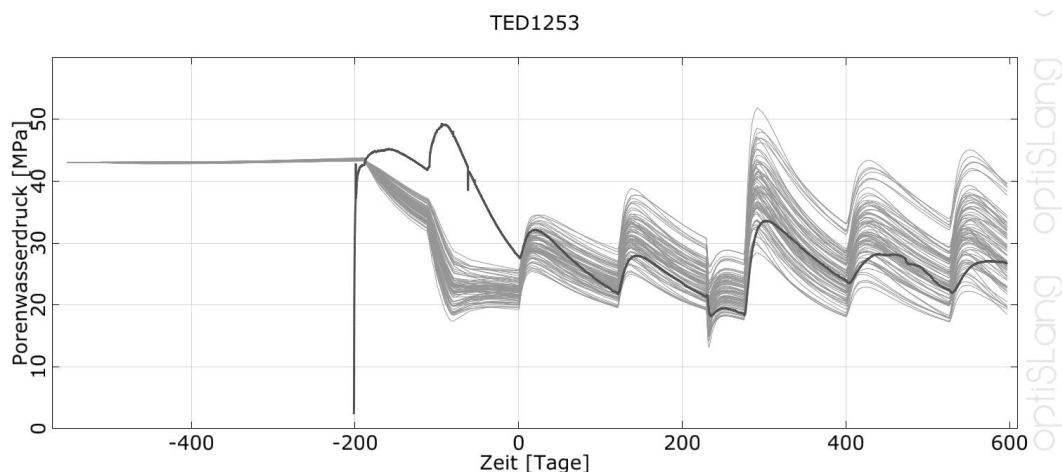


Figure 7: pore water pressure at the measurement point 1253 with a scattering range of the simulation model

6 Parameter identification

Within the parameter identification, a set of input parameters is determined which simulates decently the time evolution of the measured and calculated temperatures and pore water pressures. Parameters not affecting the response variables in the sensitivity analysis were excluded from the parameter identification. They were taken into account with their reference values. The set of the material parameters is listed in Table 1. Because the effects of initial disturbances (e.g. from tunnel excavation and installation of heating devices) decline in the course of the test, prognosis quality rises with each heating period. Therefore, the objective function for each heating periods were chosen with different priority factors (0.6 for

heating period 1, 0.8 for heating period 2 and 1.0 for heating period 3). For the calibration of measurement and simulation, besides discrete values of the sensitivity analysis (see Figure 3), also the integral differences between the measured and calculated ranges were considered. For optimization, the adaptive response surface method being available in optiSLang was used.

Material parameters		values
density	ρ (kg.m ⁻³)	2333
thermal conductivity parallel z. bedding plane	λ_p (W.m ⁻¹ .K ⁻¹)	2,02
thermal conductivity normal z. bedding plane	λ_n (W.m ⁻¹ .K ⁻¹)	1,37
specific thermal conductivity	c (J.kg ⁻¹ .K ⁻¹)	695
Constants for permeability function	$k_{0,p}$ (m ²)	5,87E-19
	n_p (-)	1,07871
	$k_{0,n}$ (m ²)	1,50E-20
	n_n (-)	0,15363
	k_e (m ²)	9,92E-15
	$k_{e,max}$ (m ²)	1,18E-16
Factor of the thermal expansion coefficient (pore fluid)	$\alpha_{f, factor}$ (-)	0,344
Porosity	n (-)	0,1646
Biot-modulus	M (Pa)	3,9E+09
Biot-constants	α (-)	0,65
Elasticity characteristics (transversal isotrop)	E_p (Pa)	8.230E+09
	E_n (Pa)	5.731E+09
	ν_p (-)	0.3
	ν_{np} (-)	0.3
	G_{np} (Pa)	2.70E+09
friction angle (rock matrix)	φ_g (°)	28,79
Dilatancy angle (rock matrix)	ψ_g (°)	28,79
Cohesion (rock matrix)	c_g (Pa)	3,794E+06
Remaining properties as coefficient based on the mechanical strength properties (Gesteinsmatrix)	$\varphi_{gr, fact}$ (-)	0,84
	$c_{gr, fact}$ (-)	0,444
tensile strength (rock matrix)	σ_{tg} (Pa)	1,30E+06
friction angle (bedding plane)	φ_l (°)	23,54
Cohesion (bedding plane)	c_l (Pa)	1,50E+06
tensile strength (bedding plane)	σ_{tl} (Pa)	0,50E+06

Table 1 Set of claystone material parameter

The comparison of the measured and calculated time signals of the temperatures and the relative pore water pressures (see Figure 8) shows the very accurate simulation of the used model concerning the observed physical phenomena (thermal-hydraulic and thermo-mechanical as well as thermo-plastic effects) in the heating experiment.

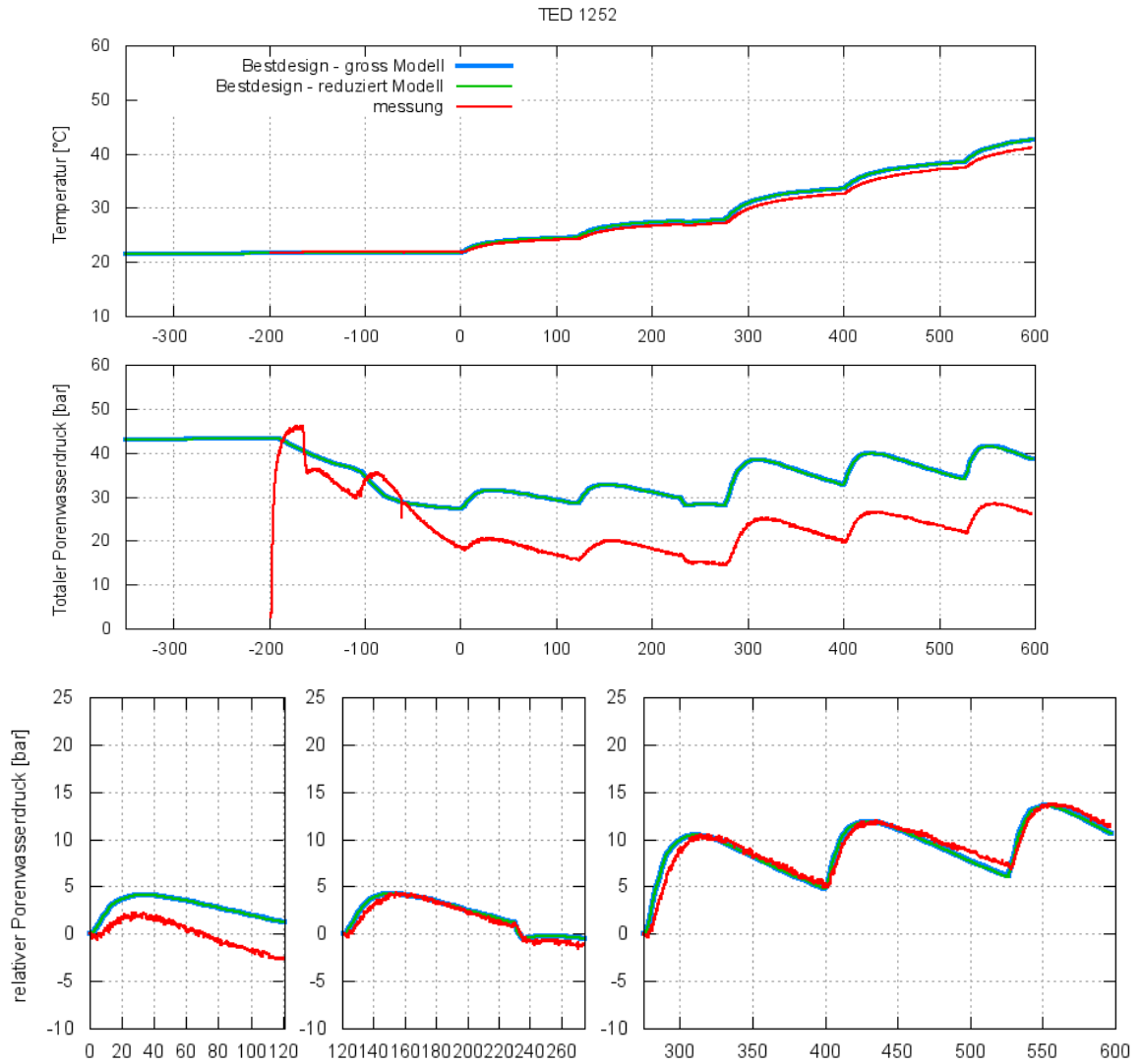


Figure 8: Comparison of simulation vs. measurement at point 1252 after the parameter identification. Top: temperature curve, middle: total pore water pressure, bottom: relative pore water pressure of the three heating periods

7 Conclusions

Based on ANSYS and multiPlas, an efficient THM-simulator was developed. The simulator computes a design completely from the tunnel excavation to the end of the third heating phase in only 32 hours on an ordinary PC workstation with two CPU. optiSlang's high-performance algorithms and filtering strategies for coping

with large parameter spaces (advanced Latin hypercube sampling, and Metamodel respectively Coefficient of best prognosis) enabled the efficient determination of significant input parameters and the evaluation of the main physical phenomena. The sensitivity analysis shows very accurately the following main influences affecting the pore water pressure before the start of the heating phase at time $t = 0$:

- hydraulic-mechanical effects, i.e. permeability due to the stress redistribution and plastic strains in the loosening zones of the tunnel excavation and heater drills
- changing of volumetric strain
- Biot modulus

Changes of the pore water pressure after the beginning and during the course of the heating are significantly influenced by:

- thermal-hydraulic coupling (strongest influence)
- hydraulic-mechanical coupling, i.e. permeability due to stress redistribution, strength characteristics of the claystone and volumetric strain changes

Using powerful optimization algorithms in optiSLang, the most important parameters for T-H-M coupled simulations in claystone (Callovo-Oxfordian) could be successfully identified. The precise simulation results of the measured and calculated differences of pressures illustrated the accurate evaluation of both the rising of the heating gradient of the pore water pressure due to the start of each heating phases and the subsequent declining gradient. The used simulation model and the T-H-M coupling proved to be capable to explain the important thermal hydraulic effects (rising pore water pressure due to temperature increase) and thermo-mechanical effects (decrease of pore pressure due to changes of stress, drainage effects and plastic activities as well as related changes in the permeability). There are plans to continue using the developed T-H-M simulator for future calculations or other identifications in the field of disposal sites research for hazardous waste in underground laboratories.

8 References/Literature

- ANDRA: Andra research on the geological disposal of high-level long-lived radioactive waste – Dossier 2005 – Results and perspectives, ANDRA, Châtenay-Malabry, France.
- GENS, A.; VAUNAT, J.; GARITTE, B.; WILEVEAU, Y.: In situ behaviour of a stiff layered clay subject to thermal loading: observations and interpretation. (2007) *Geotechnique* 57, No. 2, 207-228
- MILLARD, A. ET AL: Numerical study of the THM effects on the near-field safety of a hypothetical nuclear waste repository – BMT1 of the DECOVALEX III project. Part 2: Effects of THM coupling in continuous and homogeneous rocks. *Int. J. of Rock Mech. & Min. Sci* 42 (2005), 731-744
- MULTIPLAS – elastoplastic material models for ANSYS, version 6.0. DYNARDO GmbH, Weimar, 2010, www.dynardo.de, multiPlas user's manual
- NARASIMHAN, T.N.: Coupled equations for transient water flow, heat flow, and deformation in hydrogeological systems" *J. Earth Syst. Sci* 115, No. 2, April 2006, pp. 219-228
- OPTISLANG - the optimizing Structural Language version 3.1.4, DYNARDO GmbH, Weimar, 2010, www.dynardo.de
- WITTKÉ, W.: *Felsmechanik, Grundlagen für wirtschaftliches Bauen im Fels.* Springer-Verlag, Berlin, Heidelberg, New York, Tokyo (1984)